

ACQ: A Unified Framework for Automated Programmatic Creativity in Online Advertising

Ruizhi Wang
Huazhong university of science and
technology
Wuhan, China
wangruizhi@hust.edu.cn

Kai Liu
Kuaishou Technology
Hangzhou, China
liukai10@kuaishou.com

Bingjie Li
Kuaishou Technology
Beijing, China
libingjie03@kuaishou.com

Yu Rong
Kuaishou Technology
Beijing, China
rongyu03@kuaishou.com

Qingpeng Cai^{*}
Kuaishou Technology
Beijing, China
caiqingpeng@kuaishou.com

Fei Pan
Kuaishou Technology
Beijing, China
panfei05@kuaishou.com

Peng Jiang
Kuaishou Technology
Beijing, China
jiangpeng@kuaishou.com

Abstract

In online advertising, the demand-side platform (a.k.a. DSP) enables advertisers to create different ad creatives for real-time bidding. Intuitively, advertisers tend to create more ad creatives for a single photo to increase the probability of participating in bidding, further enhancing their ad cost. From the perspective of DSP, the following are two overlooked issues. On the one hand, the number of ad creatives cannot grow indefinitely. On the other hand, the marginal effects of ad cost diminish as the number of ad creatives increases. To this end, this paper proposes a two-stage framework named Automated Creatives Quota (ACQ) to achieve the automatic creation and deactivation of ad creatives. ACQ dynamically allocates the creative quota across multiple advertisers to maximize the revenue of the ad platform. ACQ comprises two components: a prediction module to estimate the cost of a photo under different numbers of ad creatives, and an allocation module to decide the quota for photos considering their estimated costs in the prediction module. Specifically, in the prediction module, we develop a multi-task learning model based on an unbalanced binary tree to effectively mitigate the target variable imbalance problem. In the allocation module, we formulate the quota allocation problem as a multiple-choice knapsack problem (MCKP) and develop an efficient solver to solve such large-scale problems involving tens of millions of ads. We performed extensive offline and online experiments to validate

the superiority of our proposed framework, which increased cost by 9.34%.

CCS Concepts

• **Information systems** → **Computational advertising; Decision support systems**; • **Applied computing** → **Electronic commerce**.

Keywords

E-commerce, Programmatic Creativity, Infrastructure Allocation, Online Advertising

ACM Reference Format:

Ruizhi Wang, Kai Liu, Bingjie Li, Yu Rong, Qingpeng Cai^{*}, Fei Pan, and Peng Jiang. 2024. ACQ: A Unified Framework for Automated Programmatic Creativity in Online Advertising. In *Proceedings of The Web Conference 2025 (WWW '25)*. ACM, New York, NY, USA, 10 pages. <https://doi.org/XXXXXXX.XXXXXXX>

1 Introduction

Online advertising generates substantial revenue for many Internet companies[24, 44]. Prominent Internet companies, including Google, ByteDance, Kuaishou, Tencent, and Baidu, have developed sophisticated demand-side platforms (DSPs). These platforms are instrumental in automating advertising strategy formulation, optimizing ad delivery, and facilitating real-time bidding. These highly automated and user-friendly platforms substantially enhance advertising efficacy[8, 43]. As a short video platform with nearly 400 million daily active users (DAU), Kuaishou has implemented an advanced automated advertising delivery system. In advertising systems, advertisers must set the quota ratio for three hierarchical levels within their accounts—campaigns, units, and creatives—based on their experience, as well as determine the number of creatives created from each photo. Figure 1 provides additional details.

Advertisers tend to create multiple creatives for a single photo, with each creative potentially appealing to different audiences, in

^{*}Corresponding author.

Permission to make digital or hard copies of all or part of this work for personal or classroom use is granted without fee provided that copies are not made or distributed for profit or commercial advantage and that copies bear this notice and the full citation on the first page. Copyrights for components of this work owned by others than the author(s) must be honored. Abstracting with credit is permitted. To copy otherwise, or republish, to post on servers or to redistribute to lists, requires prior specific permission and/or a fee. Request permissions from permissions@acm.org.

WWW '25, April 28–May 2, 2025, Sydney, Australia

© 2024 Copyright held by the owner/author(s). Publication rights licensed to ACM.
ACM ISBN 978-1-4503-XXXX-X/18/06
<https://doi.org/XXXXXXX.XXXXXXX>

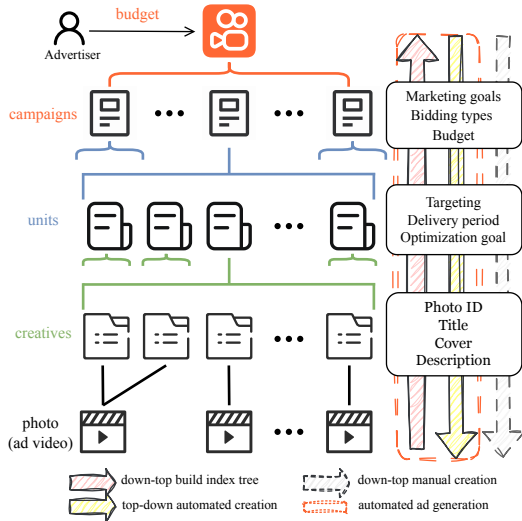


Figure 1: The hierarchical relationships within advertising. From top to bottom, these levels are campaigns, units, and creatives. A creative can be created from only one photo. However, advertisers can delegate this process to the advertising platform, which can automatically create multiple creatives from a single photo by combining different titles or themes.

order to increase ad cost[26, 27]. Assuming the cost of each photo used to create a single creative is an independent and identically distributed (iid) random variable X with an expected value $E(X)$, the total cost of a photo used to create n creatives is represented by $F(x, n)$, with an expected value $E(F(x, n)) = n \cdot E(X)$. This indicates that increasing the number of creatives created from a single photo correlates positively with total ad cost.

However, two critical issues are often overlooked from the perspective of DSPs. First, the number of creatives cannot expand indefinitely due to platform capacity limitations. Additionally, an excessive number of new creatives can result in significant data sparsity issues, as the majority may remain unconsumed. Second, in practice, the total cost $F(x, n)$ is likely a submodular function, indicating the marginal contribution of each additional creative diminishes as the number of creatives increases. This phenomenon is attributed to audience overlap among creatives, as well as the relevance and competitiveness of advertisements. This paper focuses on the automated dynamic creation and cessation of creatives with the objective of maximizing platform revenue. To the best of our knowledge, no comparable research has been conducted in the industry.

In this paper, we define *the infrastructure allocation problem* as optimizing the number of creatives created from a single photo to maximize total cost. However, several challenges arise in modeling infrastructure allocation. First, the actual cost metrics for advertising photos exhibit a significant imbalance, with over 98%

of photos experiencing no cost on a given day. This severe imbalance presents a substantial challenge for predictive modeling techniques, as conventional methods for addressing data imbalance are inadequate for such distributions. Second, traditional regression models lack interpretability and fail to capture the functional relationship between photo cost and the number of creatives, resulting in unreliable predictions in real-world scenarios. From a logical perspective, this relationship is likely to be monotonic, submodular, and smooth. Third, the total number of photos is approximately 10 million. Traditional solvers struggle with issues related to computational resources, memory requirements, and processing time when addressing ultra-large-scale optimization problems.

This paper proposes a new framework named Automated Creatives Quota (ACQ) for addressing the infrastructure allocation problem, inspired by the successful two-stage "prediction + allocation" approach employed in industries such as budget allocation[7, 12], bonus and discount allocation[6, 11], and insurance claims[10]. ACQ consists of two steps: learning the cost model of photos utilized for creating varying numbers of creatives from historical data and allocating the number of creatives to each photo based on business constraints. The prediction module models the data using an unbalanced binary tree and designs a new loss function based on multi-task learning to address the imbalance of the target variable. Cost prediction is performed through a multi-head structure, enabling the model to capture properties that align with logical deductions. The allocation module reformulates the problem as an equivalent convex optimization problem, applies the Lagrange multiplier method to find the optimal solution, and accelerates the process using the bisection method. The time complexity of each iteration is $O(n)$ [7], making it suitable for large-scale problems. Our contributions can be summarized as follows:

- We proposed a solution framework named ACQ for a new fundamental problem with significant commercial value, which has not been studied by the industry.
- We developed a multi-task learning model based on an unbalanced binary tree to effectively address the imbalance in the target variable. Furthermore, we verified the properties of network monotonicity, submodularity, and smoothness during the modeling process, enhancing the model’s interpretability.
- We utilized the Lagrange dual method with bisection to calculate the Lagrange multiplier, compress the strategy space, and solve the large-scale allocation problem involving tens of millions with high efficiency.
- We conducted extensive offline experiments on real-world datasets and online A/B experiments in real business scenarios. The results demonstrated the superiority of ACQ.

The rest of our paper is organized as follows. We introduce related work in Section 2 and briefly formulates infrastructure allocation problem in Section 3. In Section 4, we introduce the proposed framework. We presents the dataset, offline experiments, and online experiments in Section 5. The conclusions are given in Section 6.

2 Related Work

Programmatic Creativity Commercial advertising generates substantial profits for enterprises and has become an integral component of corporate marketing strategies[1]. The advertising platform’s delivery process is divided into the production and editing of campaigns, units, and creatives. The integration of AI in the advertising sector enhances the personalization, precision, and intelligence of advertisements[2]. In the creative dimension, AI applications primarily encompass two key areas: dynamic creative optimization (DCO) and programmatic advertising creation (PAC)[1]. DCO is a technology that leverages data and algorithms to create and optimize advertising creative in real time. By analyzing data such as user behavior, interests, and environmental factors, DCO can automatically adjust advertising content to better align with the needs and preferences of the target audience[3, 4]. PAC involves the automatic creation of ad creativity through programmatic methods. It utilizes technologies such as machine learning and natural language processing to select and combine the most appropriate elements from an extensive library of materials to produce high-quality advertising content[5].

Deep Imbalanced Regression Learning from imbalanced data using neural networks remains a challenging research problem[13, 32]. Single-stage methods typically involve oversampling, under-sampling, or reweighting the loss function during training. Multi-stage methods enhance long-tail predictions by decoupling the learning of representations from the learning of classifier heads. However, these methods lack generalizability and require extensive hyperparameter tuning[14]. Long-tail data is a significant characteristic in short video recommendation business scenarios. In this domain, certain models based on multi-task learning[15] have partially mitigated the challenges posed by data distribution. For instance, employing interval quantiles as labels[16] and modeling multiple binary classification problems[17] have proven beneficial for addressing imbalanced data. Significantly, several approaches integrating neural networks with tree-based models have demonstrated remarkable efficacy. TPM[18] employs viewing time prediction as an estimate of the expected ordinal rank and proposes a decomposition tree search to replace the traditional linear search.

Network Property Modeling Modeling network properties within neural network models is essential across various practical domains. For example, in finance, the conversion rate for the same user under varying privileges increases as the privileges increase[11, 12]. Ensuring the monotonicity of neural networks involves either function modeling or the design of loss functions and neural network architectures. Function modeling entails establishing a priori linear[6] or nonlinear monotonicity[7, 8] functions based on data distribution and employing models to estimate the parameters corresponding to these functions. The design of loss functions involves the common pair-wise loss in ranking tasks, which is based on the relative order between data point pairs[9]. In model design, selecting an appropriate activation function is crucial for maintaining monotonicity in feature encoding and transformation. Additionally, the activation function of the estimation layer must be monotonic, non-negative, and concave[10]. A direct approach entails designing a neural network with multiple output

heads, where each head predicts the increment relative to its predecessor. Activation functions such as square or exponential can be employed to ensure that the increment is positive[11, 12].

Lagrangian dual method One of the most effective methods for decision-making in the second stage is the Lagrangian dual method. Li et al.[23] and Ai et al.[19] modeled the decision-making problem as a multiple choice knapsack problem (MCKP)[45], constructed a Lagrangian relaxation function, and utilized a dual gradient descent method. Zhao et al.[7] and Wang et al.[11] implemented an efficient algorithm based on the bisection method for solving the MCKP. Wu et al.[10] approached the online constrained submodular welfare maximization (SWM) problem, aiming to maximize fraud detection accuracy. The PDA-SP algorithm was proposed to expedite the solution of the dual problem by leveraging submodularity and piecewise linear properties.

3 Problem Formulation

In this section, we formulate the infrastructure allocation problem as a multiple choice knapsack problem (MCKP). Specifically, the task involves determining the optimal number of creatives to be created from each photo. This task constitutes a constrained optimization problem. The objective is to maximize the estimated cost of all photos, subject to a constraint on the total number of creatives. We formulate this optimization problem as follows:

$$\begin{aligned}
 \max \quad & \sum_{i=1}^I \sum_{j=1}^J \sum_{k=1}^K r_{ijk} x_{ijk} \\
 \text{s.t.} \quad & \sum_{i=1}^I \sum_{j=1}^J \sum_{k=1}^K c_k x_{ijk} \leq C \\
 & \sum_{k=1}^K x_{ijk} = 1, \quad \forall i, j \\
 & x_{ijk} \in \{0, 1\}, \quad \forall i, j, k \\
 & c_k = 1, 2, \dots, 200
 \end{aligned} \tag{1}$$

where for a given account-photo ID pair (i, j) , k denotes the number of creative candidates for the account-photo ID pair, and c_k represents the number of photos used to create candidate k . In practical applications, a photo can be used to create up to 200 creatives. x_{ijk} represents the account-photo ID pair created by k creatives, and r_{ijk} denotes the cost of the pair. r_{ijk} is calculated as shown in Equation 2, where $pvalue_{ijk}$ is the output of the first stage of the ACQ, representing the estimated cost of the account-photo ID pair used for creating k creatives.

$$r_{ijk} = pvalue_{ijk} + \lambda \cdot explore_score_{ijk} \tag{2}$$

where $explore_score_{ijk}$ represents the exploration score, based on the classic UCB algorithm in reinforcement learning[41]. It scores each photo based on past statistical experience and uncertainty. In actual business, it plays a significant role in balancing exploration and utilization.

4 Methodology

In this section, we present the details of ACQ. In the prediction module, we address the challenge of unbalanced target variables and

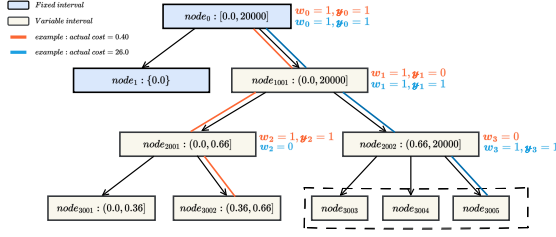


Figure 2: Binary tree modeling on real-world datasets. The leaf nodes may prevent the entire structure from being a strict binary tree due to the significant long-tail distribution and the overlap of quantiles, which result in indivisible sub-intervals.

examine network properties to ensure monotonicity, submodularity, and smoothness. In the allocation module, we tackle the large-scale allocation problem using a Lagrangian dual optimization method with bisection.

4.1 Prediction Module

4.1.1 Modeling based on unbalanced binary tree. Given a training set (X, n, C) , where X denotes the features of the photo, n represents the number of creatives created from the photo, and C indicates the actual cost. The objective of the first stage is to construct a model M that accurately fits the data distribution of the training set. Additionally, this stage aims to mitigate challenges associated with the model’s prediction results $M(X|c)$, which may exhibit bias towards high-frequency values or display imbalanced evaluation metrics due to the inherent imbalance in target variables[32].

Datasets in recommendation systems often exhibit a long-tail distribution, where tree-based neural networks like TDM[31] and TPM[18] perform strongly. Inspired by these models, we propose a modeling approach called Unbalanced Binary Tree Model (UBTM), which is based on an unbalanced binary tree. For the sample set, we construct an unbalanced binary tree T consisting of N nodes, each representing an interval or point set of cost, as illustrated in Figure 2. Assuming there are m training samples, with the cost of each sample x_i denoted as y_i , the cost should satisfy $\{y_0 \leq y_1, \dots, y_k, \dots, \leq y_m\}$ after being sorted in ascending order. The root node $node_0$ then represents the full interval of the cost, i.e., $node_0 \in [y_0, y_m]$. The left child $node_1$ of the root node represents the $\{0\}$ set, i.e., the sample with $y_i = 0$; these two sets remain unchanged regardless of the data distribution of the training dataset, whereas the right subtree of the root node adapts accordingly. In the right subtree of the root node, each leaf node represents a data interval formed by equally frequent grouping of samples with $y_i > 0$, and the subspace of the parent node is the union of the subspaces of its child nodes.

In the model, each non-leaf node is equipped with a binary classifier. If the unbalanced binary tree has N_f leaf nodes, then it contains $N - N_f$ binary classifiers. The output of a non-leaf node represents the conditional probability that the cost belongs to the interval or point set associated with the child node, based on the output probability of its parent node. In other words, for any node in T , we must determine the path p_{ℓ} from the root node

to it and multiply the probability outputs of multiple classifiers. Consequently, given the node $node_{\ell}$ at the $d(\ell)$ -th layer, its cost follows the subsequent multinomial distribution:

$$p(C \in node_{\ell} | X, T) = \begin{cases} p(C = 0 | X, T) & \text{if } node_{\ell} = \{0\} \\ p(C \in \mathcal{P}_{d(\ell)}(\ell) | X, T) & \text{otherwise} \end{cases} \quad (3)$$

where $\mathcal{P}_i(\ell)$ denotes the node at the i -th level ($i \in \{0, 1, 2, \dots\}$) on the path from the root node to $node_{\ell}$ ($d(\ell) \gg 1$). Then, $p(C \in \mathcal{P}_{d(\ell)}(\ell) | X, T)$ represents the conditional probability of $\mathcal{P}_i(\ell)$. Consequently, we can infer:

$$\begin{aligned} p(C \in node_{\ell} | X, T) &= p(C \in \mathcal{P}_{d(\ell)}(\ell) | X, T) \\ &= \prod_{i=1}^{d(\ell)} p(C \in \mathcal{P}_i(\ell) | X, T, C \in \mathcal{P}_{i-1}(\ell)) \end{aligned} \quad (4)$$

For a leaf node $node_{\ell}$, its conditional probability represents the likelihood of the cost falling within the corresponding interval. Certain approaches estimate the metric by accumulating the products of each leaf node interval’s midpoint value and its associated conditional probability. However, if the range of a leaf node interval is too large (e.g., $(46.37, 20000]$), it can significantly affect the regression value. Therefore, the unbalanced binary tree we constructed will be used for auxiliary tasks in multi-task learning.

4.1.2 Multi-task learning. Multi-task learning[33] effectively leverages shared information among related tasks to enhance the model’s generalization capability. The model trains $N - N_f$ binary classification tasks, where $N - N_f$ represents the number of non-leaf nodes in an unbalanced binary tree. Each binary classification task computes the conditional probability of a cost falling within the interval represented by the corresponding child node, conditioned on the parent node’s output. The classification error component aims to maximize the likelihood of a sample belonging to the leaf node along its traversal path. To quantify the discrepancy between predicted and actual probability distributions, we employ the cross-entropy loss function:

$$l_1 = \sum_{i=1}^{N-N_f} w_i (-y_i \log \hat{y}_i - (1 - y_i) \log(1 - \hat{y}_i)) \Big|_{node_i \notin S_{\text{leaf}}} \quad (5)$$

where S_{leaf} denotes the set of leaf nodes. \hat{y}_i denotes the estimated value of the model classifier, while y_i represents the actual binary label of the sample, determined by the sample’s cost and the range of each interval in the unbalanced binary tree T . Before training commences, each sample is assigned to a leaf node of T . The traversal path from the root node to the leaf node determines the y_i value of the sample. The classifier weight w_i along this path is set to 1, serving as a mask, while it is set to 0 for all other paths. Figure 2 illustrates two examples of this process.

An additional auxiliary task involves quantifying uncertainty. By integrating the standard deviation into the loss function, the model can emphasize not only prediction accuracy but also confidence, thereby enhancing the overall reliability of the predictions[18]. Note that C represents the total estimated cost:

In our model, the effect increment slope y''_i can be interpreted as the average rate of change over the interval, equivalent to $f'(c)$. This reasoning enables us to derive the form of Equation 11.

Smoothness. DEFINITION: *The change in total cost should be smooth as the number of creatives increases. This can be ensured by Lipschitz continuity: $\forall n_1, n_2 \in \{1, 2, \dots, 200\}$, $|cc_{n_1} - cc_{n_2}| \leq L|n_1 - n_2|$, where L is a Lipschitz constant ensuring the smoothness of the cost function.*

Smoothness is a crucial attribute that ensures the function does not exhibit abrupt changes, which would be impractical for real-world applications[12]. To incorporate smoothness into our model, we estimate the Lipschitz constant z_j for the j -th layer by calculating the spectral norm (i.e., the largest singular value) of the weight matrix of that layer. Subsequently, the Lipschitz constant of the entire network can be approximated by the product of the Lipschitz constants of each layer[36, 37]. Finally, this overall Lipschitz constant is incorporated into the loss function as a regularization term. The Lipschitz-regularized loss function l_{lip} and the total loss of the network $l_{\text{smoothness}}$ are expressed as follows:

$$l_{\text{lip}} = \prod_{j=1}^L \text{softplus}(z_j) \quad (14)$$

$$l_{\text{smoothness}} = l + \lambda l_{\text{lip}} \quad (15)$$

where $\text{softplus}(z_j) = \ln(1 + e^{z_j})$ is utilized to ensure the non-negativity of z_j , L denotes the number of fully connected layers, and λ is a weighting coefficient that modulates the intensity of the smoothness regularization constraint.

4.2 Allocation Module

Integer programming problems, especially large-scale ones, are inherently complex and computationally expensive. In contrast, linear programming problems can be solved in polynomial time, with optimal solutions readily obtainable through existing efficient algorithms[38]. Previously, we formulated the infrastructure allocation problem as an optimization problem, as shown in Equation 1. To expedite the solution process, we relax this problem into a linear programming problem by allowing the variable x_{ijk} to take values in the continuous interval $[0, 1]$ instead of the discrete set $\{0, 1\}$. The corresponding relaxed problem is formulated as follows:

$$\begin{aligned} \max \quad & \sum_{i=1}^I \sum_{j=1}^J \sum_{k=1}^K r_{ijk} x_{ijk} \\ \text{s.t.} \quad & \sum_{i=1}^I \sum_{j=1}^J \sum_{k=1}^K c_k x_{ijk} \leq C \\ & \sum_{k=1}^K x_{ijk} = 1, \quad \forall i, j \\ & c_k = 1, 2, \dots, 200 \end{aligned} \quad (16)$$

Strong Duality Theorem: *For a convex optimization problem, if certain conditions (e.g., Slater's condition) are satisfied, the optimal value of the primal problem equals that of the dual problem.*

The relaxed problem is a linear programming problem that satisfies both strong duality and the Karush-Kuhn-Tucker (KKT) conditions. By introducing the constraint $\sum_{i,j} \sum_k c_k x_{ijk} \leq C$ with its

corresponding Lagrange multiplier $\lambda > 0$, we derive the Lagrangian form of Problem 16 as follows:

$$\max_X L(X, \lambda) = \sum_{ij} \sum_k r_{ijk} x_{ijk} + \lambda \left(C - \sum_{ij} \sum_k c_k x_{ijk} \right) \quad (17)$$

The dual problem of the original problem entails minimizing the Lagrangian function. Formally, it can be expressed as follows:

$$\min_{\lambda} \max_X L(X, \lambda) = \sum_{ij} \sum_k r_{ijk} x_{ijk} + \lambda \left(C - \sum_{ij} \sum_k c_k x_{ijk} \right) \quad (18)$$

One of the KKT conditions for obtaining the optimal solution is complementary slackness, which states:

$$\lambda \left(C - \sum_{ij} \sum_k c_k x_{ijk} \right) = 0 \quad (19)$$

PROPOSITION 1: *Given the dual variable λ , for each i and j , the optimal k^* is determined by $k^* = \arg \max_k (r_{ijk} - \lambda c_k)$. Consequently, $x_{ijk^*} = 1$.*

Based on Proposition 1, the problem is reformulated to focus on determining the dual variable λ . We denote the partial expression on the right-hand side of Equation 19 by $g(\lambda)$:

$$g(\lambda) = \sum_{ij} \sum_k c_k * x_{ijk} - C \quad (20)$$

PROPOSITION 2: *The function $g(\lambda) = \sum_{ij} \sum_k c_k \cdot x_{ijk} - C$ is a monotone non-increasing function of λ .*

According to Proposition 2, the function $g(\lambda)$ is monotonic. As stated in Equation 19, the corresponding λ is optimal when $g(\lambda) = 0$. Therefore, we employ a method called Dual based Binary Search Solver (DBSSolver), which utilizes a binary search approach to determine the optimal value of λ [7]. Once this optimal λ is found, we solve the optimization problem presented in Equation 17. This conclusion is substantiated in Proposition 1.

5 Experiments

5.1 Dataset

The real-world dataset used in this study is sourced from Kuaihou's advertising intelligent delivery platform. A detailed description is provided in Table 1.

Table 1: Dataset Statistics

Data Size	Mean	Median	Std Dev	Min	Max
60M	0.81	0.00	40.10	0.00	20000.00
sparse feature	"product name", "first industry name" "second industry name"				
dense feature	Statistical values of "creative cost", "target cost", "creative conversion", "creative impression" in different time windows				

5.2 Offline Experiments

To demonstrate the effectiveness of the ACQ, experiments were conducted separately on the prediction and allocation modules. The training and validation data were obtained from two consecutive days within the real-world dataset.

5.2.1 Prediction.

Comparison Methods.

- **UBTM**: The model we proposed is a multi-task learning framework based on an unbalanced binary tree, as shown in Figure 5.
- **DNN**: The basic regression model utilizes a deep neural network for prediction, employing the Mean Squared Error (MSE) loss function, as illustrated by structure l_3 in Figure 3.
- **ZILN**[39]: This approach employs a deep neural network in conjunction with the Zero-Inflated Log-Normal (ZILN) loss function for lifetime value (LTV) prediction. The ZILN loss function combines a zero-point mass with a log-normal distribution to address challenges related to zero-value occurrences and long-tail distributions in LTV prediction.
- **CREAD**[17]: The CREAD framework initially discretizes the continuous label into multiple intervals. Subsequently, it trains multiple binary classifiers to predict whether the viewing time exceeds each threshold. Finally, the framework reconstructs the final label using the predicted values from these classifiers.

Evaluation Metrics.

- **Area Under the Curve (AUC)**: AUC indicates the probability that a randomly selected positive instance is ranked higher than a randomly selected negative instance. A higher AUC signifies better model performance and serves as the core indicator in our offline experiments.
- **Mean Squared Error (MSE)**: MSE is a standard metric for regression tasks that measures the average of the squared errors between predicted and actual values. A lower MSE signifies better model performance.
- **Positive AUC (PAUC)**: PAUC is a variant of AUC focusing solely on ranking positive instances. It measures the probability that a randomly selected positive instance is ranked higher than another positive instance. A higher PAUC signifies better model performance in ranking positive instances.
- **Cost-weighted AUC (GAUC)**: GAUC extends the AUC metric by weighting it according to the total cost within each account. This approach enhances the influence of high-value accounts, as these accounts significantly contribute to online performance.

Experimental conclusion. Table 2 presents the effect of the prediction module on the real-world dataset, where "mon," "sub," and "smo" denote the monotonicity, submodularity, and smoothness structures of the model, respectively, and "control" indicates the absence of special function design. The results reveal the following observations: (1) UBTM demonstrates excellent performance in core indicators and ranks well in other metrics, proving the effectiveness of the proposed method. (2) A horizontal comparison between UBTM and DNN methods reveals that UBTM achieves

Table 2: Competitive analysis of solutions

Main Method	Variant	AUC↑	MSE↓	PAUC↑	GAUC↑
UBTM	control	0.926627	812.98	0.745376	0.682656
	mon	0.930778	852.23	0.736744	0.675737
	sub	0.933521	783.63	0.745545	0.688466
	smo	0.924065	749.76	0.725943	0.663382
DNN	control	0.884369	820.91	0.740429	0.689695
	mon	0.904987	777.41	0.741367	0.678157
	sub	0.905742	885.67	0.741194	0.682286
	smo	0.906678	821.62	0.740722	0.682286
ZILN[39]	-	0.927180	NAN*	0.240395	0.653189
CREAD[17]	-	0.806779	980.21	0.573294	0.623219

*indicates that extremely large predicted values result in NaN when squared.

Table 3: Comparison of Solvers

Solver	Dataset Size	Dual Value	Time
GLPK Solver	100k	0.0006331575705724	1.16h
	200k	0.0006331154967055	5.20h
	500k	0.0006330545772524	36.24h
DBSSolver	100k	0.0006332397460937	109.84s
	200k	0.0006332397460937	110.43s
	500k	0.0006332397460937	116.29s

significant advantages, demonstrating the benefits of modeling data distribution based on unbalanced binary trees. (3) UBTM integrates monotonicity and submodularity in model design. Ablation experiments indicate that these special designs enhance the modeling of properties and improve interpretability. However, incorporating smoothness into UBTM does not enhance performance. We hypothesize that this is due to the discretization of the number of creatives into a relatively small number of bins (9 in the actual business), resulting in mutation points in the function, which aligns with expectations.

Parameter sensitivity. As illustrated in Figure 5, multiple offline experiments were conducted by varying the weight factor of multi-task learning and modifying the number of leaf nodes in the construction of the unbalanced binary tree.

5.2.2 Allocation. We demonstrate the efficiency of the DBSSolver in providing solutions. GLPK (GNU Linear Programming Kit) is an open-source software package designed for solving large-scale linear programming, mixed integer programming, and other related problems[40]. Compared to GLPK, DBSSolver significantly enhances solution efficiency while maintaining acceptable solution quality across varying dataset sizes. The comparison results are presented in Table 3. The results further demonstrate that the dual problem can be solved by sampling large-scale instances, allowing decisions to be made on all samples based on the solved dual value to obtain the original solution, facilitated by the efficient dichotomy method.

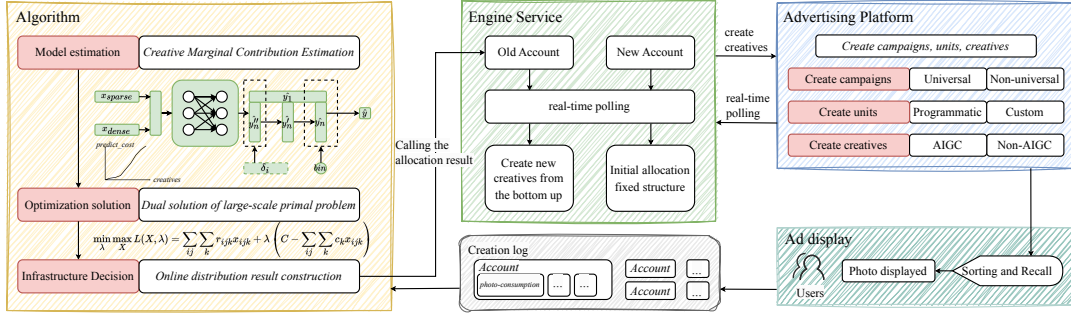


Figure 4: The actual online operation framework.

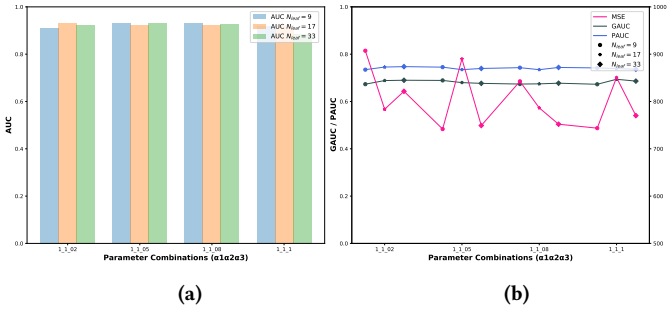


Figure 5: Parameter sensitivity experiments.

Table 4: Offline allocation results

Date	Framework	Number of Creatives (k)	Cost (k)
Day1	rule-based	621,447	37,987
	ACQ	619,721 (-0.27%)	40,843 (+7.51%)
Day2	rule-based	643,823	32,042
	ACQ	644,660 (+0.13%)	34,119 (+6.48%)
Day3	rule-based	639,766	21,457
	ACQ	629,576 (-1.59%)	22,911 (+6.78%)

Furthermore, we compare the allocation results of the rule-based strategy with those of ACQ on offline datasets under various constraints. In ACQ, the prediction module initially outputs the expected cost for each photo within each creative number category. Subsequently, allocation decisions are made in the second stage based on these predictions. The results in Table 4 demonstrate that ACQ created a similar number of creatives while increasing the total expected cost. The result suggests that ACQ is more efficient in resource allocation, leading to better utilization of the available budget while maintaining or enhancing overall performance.

5.3 Online Experiments

5.3.1 Online framework. The entire online framework is shown in Figure 4.

- **Two-stage algorithm:** This approach employs a two-stage solution of "prediction + allocation" specifically designed for

the infrastructure problem. The material creation rules at the output account granularity are stored in Redis.

- **Engine service:** On the engine side, the service retrieves the creation rules from Redis in real-time for existing accounts, ensuring that the online infrastructure volume of account materials aligns with the synchronized rules.
- **Advertising platform:** The ad platform determines the optimal number of creatives that should be created for each photo based on the algorithm module. Subsequently, the platform allocates all creatives from campaigns to units, then constructs a complete three-level index tree for each account.
- **Ad Display:** The process of advertisement display involves recall, rough sorting, and fine sorting, and is completed after matching with user-side features, resulting in an increased cost of photos[42].

5.3.2 A/B test. ACQ has been implemented on the Kuaishou advertising platform, where we conducted A/B testing over a period of 6 days, focusing on actual cost and the number of creatives. Compared to Kuaishou’s existing rule-based baseline, ACQ increases cost by an average of 9.34% and the total number of creatives by an average of 1.42%, indicating a significant improvement. This demonstrates that a more intelligent infrastructure allocation is achieved while adhering to the specified constraints.

6 Conclusion

In this paper, we present a two-stage framework named ACQ for addressing a fundamental challenge: optimizing the number of creatives created from a single photo to maximize total cost. The initial stage employs UBTM, a cost prediction model leveraging unbalanced binary trees for multi-task learning in data modeling. UBTM incorporates network components ensuring monotonicity and submodularity, thereby guaranteeing accurate and interpretable outputs. The subsequent stage utilizes a Lagrangian root-finding module coupled with DBSSolver, which employs a dichotomy method. DBSSolver substantially expedites the solution process compared to conventional solvers, rendering it appropriate for high-traffic, real-world scenarios. ACQ, characterized by its simplicity, has been successfully implemented on the Kuaishou Magnetic Engine advertising platform. Comprehensive offline experiments and online A/B tests have corroborated its efficacy.

References

- [1] G. Chen, P. Xie, J. Dong, and T. Wang, "Understanding programmatic creative: The role of ai," *Journal of Advertising*, vol. 48, no. 4, pp. 347–355, 2019.
- [2] J. Ford, V. Jain, K. Wadhvani, and D. G. Gupta, "Ai advertising: An overview and guidelines," *Journal of Business Research*, vol. 166, p. 114124, 2023.
- [3] L. Baardman, E. Fata, A. Pani, and G. Perakis, "Dynamic creative optimization in online display advertising," Available at SSRN 3863663, 2021.
- [4] Y. Koren, O. Somekh, A. Shahar, A. Itzhaki, T. Cohen, M. Krasteva, and T. Shadi, "Dynamic creative optimization in verizon media native advertising," in *2020 IEEE International Conference on Big Data (Big Data)*. IEEE, 2020, pp. 1654–1662.
- [5] S. Guo, Z. Jin, F. Sun, J. Li, Z. Li, Y. Shi, and N. Cao, "Vinci: an intelligent graphic design system for generating advertising posters," in *Proceedings of the 2021 CHI conference on human factors in computing systems*, 2021, pp. 1–17.
- [6] Z. Liu, D. Wang, Q. Yu, Z. Zhang, Y. Shen, J. Ma, W. Zhong, J. Gu, J. Zhou, S. Yang *et al.*, "Graph representation learning for merchant incentive optimization in mobile payment marketing," in *Proceedings of the 28th ACM International Conference on Information and Knowledge Management*, 2019, pp. 2577–2584.
- [7] K. Zhao, J. Hua, L. Yan, Q. Zhang, H. Xu, and C. Yang, "A unified framework for marketing budget allocation," in *Proceedings of the 25th ACM SIGKDD International Conference on Knowledge Discovery & Data Mining*, 2019, pp. 1820–1830.
- [8] X. Chen, Z. Liu, L. Yu, S. Li, L. Gu, X. Zeng, Y. Tan, and J. Gu, "Adversarial learning for incentive optimization in mobile payment marketing," in *Proceedings of the 30th ACM international conference on information & knowledge management*, 2021, pp. 2940–2944.
- [9] R. Chin, C. Manzie, A. Ira, D. Nestic, and I. Shames, "Gaussian processes with monotonicity constraints for preference learning from pairwise comparisons," in *2018 IEEE Conference on Decision and Control (CDC)*. IEEE, 2018, pp. 1150–1155.
- [10] Y. Wu, Z. Zhu, C. Ma, H. Qian, X. Lu, Y. Zhang, X. Qin, B. Fei, J. Zhou, and A. Zhou, "Cost-efficient fraud risk optimization with submodularity in insurance claim," in *Proceedings of the 30th ACM SIGKDD Conference on Knowledge Discovery and Data Mining*, 2024, pp. 3448–3459.
- [11] C. Wang, X. Shi, S. Xu, Z. Wang, Z. Fan, Y. Feng, A. You, and Y. Chen, "A multi-stage framework for online bonus allocation based on constrained user intent detection," in *Proceedings of the 29th ACM SIGKDD Conference on Knowledge Discovery and Data Mining*, 2023, pp. 5028–5038.
- [12] Z. Sun, H. Yang, D. Liu, Y. Weng, X. Tang, and X. He, "End-to-end cost-effective incentive recommendation under budget constraint with uplift modeling," in *Proceedings of the 18th ACM Conference on Recommender Systems (RecSys '24)*. Bari, Italy: ACM, October 14–18 2024, p. 10.
- [13] C. D. Alvis and S. Seneviratne, "A survey of deep long-tail classification advancements," *ACM Comput. Surv.*, vol. 1, no. 1, p. 35, April 2024.
- [14] S. Zhang, Z. Li, S. Yan, X. He, and J. Sun, "Distribution alignment: A unified framework for long-tail visual recognition," in *CVPR*, 2021.
- [15] M. Crawshaw, "Multi-task learning with deep neural networks: A survey," *ArXiv*, vol. abs/2009.09796, 2020.
- [16] R. Zhan, C. Pei, Q. Su, J. Wen, X. Wang, G. Mu, D. Zheng, P. Jiang, and K. Gai, "Deconfounding duration bias in watch-time prediction for video recommendation," in *Proceedings of the 28th ACM SIGKDD Conference on Knowledge Discovery and Data Mining*, 2022, pp. 4472–4481.
- [17] J. Sun, Z. Ding, X. Chen, Q. Chen, Y. Wang, K. Zhan, and B. Wang, "Cread: A classification-restoration framework with error adaptive discretization for watch time prediction in video recommender systems," in *Proceedings of the AAAI Conference on Artificial Intelligence*, vol. 38, no. 8, 2024, pp. 9027–9034.
- [18] X. Lin, X. Chen, L. Song, J. Liu, B. Li, and P. Jiang, "Tree based progressive regression model for watch-time prediction in short-video recommendation," in *Proceedings of the 29th ACM SIGKDD Conference on Knowledge Discovery and Data Mining*, 2023, pp. 4497–4506.
- [19] M. Ai, B. Li, H. Gong, Q. Yu, S. Xue, Y. Zhang, Y. Zhang, and P. Jiang, "Lbcf: A large-scale budget-constrained causal forest algorithm," in *Proceedings of the ACM Web Conference 2022*, 2022, pp. 2310–2319.
- [20] H. Zhou, S. Li, G. Jiang, J. Zheng, and D. Wang, "Direct heterogeneous causal learning for resource allocation problems in marketing," in *Proceedings of the AAAI Conference on Artificial Intelligence*, vol. 37, no. 4, 2023, pp. 5446–5454.
- [21] J. Albert and D. Goldenberg, "E-commerce promotions personalization via online multiple-choice knapsack with uplift modeling," in *Proceedings of the 31st ACM International Conference on Information & Knowledge Management*, 2022, pp. 2863–2872.
- [22] Z. Wu, L. Wang, F. Huang, L. Zhou, Y. Song, C. Ye, P. Nie, H. Ren, J. Hao, R. He *et al.*, "A framework for multi-stage bonus allocation in meal delivery platform," in *Proceedings of the 28th ACM SIGKDD Conference on Knowledge Discovery and Data Mining*, 2022, pp. 4195–4203.
- [23] L. Li, L. Sun, C. Weng, C. Huo, and W. Ren, "Spending money wisely: Online electronic coupon allocation based on real-time user intent detection," in *Proceedings of the 29th ACM International Conference on Information & Knowledge Management*, 2020, pp. 2597–2604.
- [24] H. Choi, C. F. Mela, S. R. Balseiro, and A. Leary, "Online display advertising markets: A literature review and future directions," *Information Systems Research*, vol. 31, no. 2, pp. 556–575, 2020.
- [25] J. Chen, J. Xu, G. Jiang, T. Ge, Z. Zhang, D. Lian, and K. Zheng, "Automated creative optimization for e-commerce advertising," in *Proceedings of the Web Conference 2021*, 2021, pp. 2304–2313.
- [26] J. Azimi, R. Zhang, Y. Zhou, V. Navalpakkam, J. Mao, and X. Fern, "The impact of visual appearance on user response in online display advertising," in *Proceedings of the 21st international conference on World Wide Web*, 2012, pp. 457–458.
- [27] Z. Zhao, L. Li, B. Zhang, M. Wang, Y. Jiang, L. Xu, F. Wang, and W. Ma, "What you look matters? offline evaluation of advertising creatives for cold-start problem," in *Proceedings of the 28th ACM international conference on information and knowledge management*, 2019, pp. 2605–2613.
- [28] P. Branco, L. Torgo, and R. P. Ribeiro, "A survey of predictive modeling on imbalanced domains," *ACM computing surveys (CSUR)*, vol. 49, no. 2, pp. 1–50, 2016.
- [29] G. E. D. A. P. Alves, D. F. Silva, R. C. Prati *et al.*, "An experimental design to evaluate class imbalance treatment methods," in *2012 11th International Conference on Machine Learning and Applications*, vol. 2. IEEE, 2012, pp. 95–101.
- [30] H. Kaur, H. S. Pannu, and A. K. Malhi, "A systematic review on imbalanced data challenges in machine learning: Applications and solutions," *ACM computing surveys (CSUR)*, vol. 52, no. 4, pp. 1–36, 2019.
- [31] H. Zhu, X. Li, P. Zhang, G. Li, J. He, H. Li, and K. Gai, "Learning tree-based deep model for recommender systems," in *Proceedings of the 24th ACM SIGKDD international conference on knowledge discovery & data mining*, 2018, pp. 1079–1088.
- [32] Y. Yang, K. Zha, Y. Chen, H. Wang, and D. Katabi, "Delving into deep imbalanced regression," in *International conference on machine learning*. PMLR, 2021, pp. 11 842–11 851.
- [33] Y. Zhang and Q. Yang, "An overview of multi-task learning," *National Science Review*, vol. 5, no. 1, pp. 30–43, 2018.
- [34] A. Kendall, Y. Gal, and R. Cipolla, "Multi-task learning using uncertainty to weigh losses for scene geometry and semantics," in *Proceedings of the IEEE conference on computer vision and pattern recognition*, 2018, pp. 7482–7491.
- [35] R. Guo and Z. Jiang, "Optimal dynamic advertising policy considering consumer ad fatigue," *Decision Support Systems*, vol. 187, p. 114323, 2024.
- [36] C. Szegedy, W. Zaremba, I. Sutskever, J. Bruna, D. Erhan, I. Goodfellow, and R. Fergus, "Intriguing properties of neural networks," in *International Conference on Learning Representations*, 2014.
- [37] H. Gouk, E. Frank, B. Pfahringer, and M. J. Cree, "Regularisation of neural networks by enforcing lipschitz continuity," *Machine Learning*, vol. 110, pp. 393–416, 2021.
- [38] N. Karmarkar, "A new polynomial-time algorithm for linear programming," in *Proceedings of the sixteenth annual ACM symposium on Theory of computing*, 1984, pp. 302–311.
- [39] X. Wang, T. Liu, and J. Miao, "A deep probabilistic model for customer lifetime value prediction," *arXiv preprint arXiv:1912.07753*, 2019.
- [40] U. Dedović and B. Gušavac, "Optimal vehicle routing in consumer goods distribution: A gnu linear programming kit-based analysis," *Acadlore Trans. Appl. Math. Stat.*, vol. 1, pp. 87–95, 2023.
- [41] P. Auer, "Finite-time analysis of the multiarmed bandit problem," 2002.
- [42] X. Yi, J. Yang, L. Hong, D. Z. Cheng, L. Heldt, A. Kumthekar, Z. Zhao, L. Wei, and E. Chi, "Sampling-bias-corrected neural modeling for large corpus item recommendations," in *Proceedings of the 13th ACM conference on recommender systems*, 2019, pp. 269–277.
- [43] L. Guo, J. Jin, H. Zhang, Z. Zheng, Z. Yang, Z. Xing, F. Pan, L. Niu, F. Wu, H. Xu *et al.*, "We know what you want: An advertising strategy recommender system for online advertising," in *Proceedings of the 27th ACM SIGKDD Conference on Knowledge Discovery & Data Mining*, 2021, pp. 2919–2927.
- [44] X. Wang, Y. Guo, H. Sheng, P. Lv, C. Zhou, W. Huang, S. Ta, D. Huang, X. Yang, L. Xu *et al.*, "Know in advance: Linear-complexity forecasting of ad campaign performance with evolving user interest," in *Proceedings of the 30th ACM SIGKDD Conference on Knowledge Discovery and Data Mining*, 2024, pp. 5926–5937.
- [45] H. Kellerer, U. Pferschy, D. Pisinger, H. Kellerer, U. Pferschy, and D. Pisinger, "The multiple-choice knapsack problem," *Knapsack problems*, pp. 317–347, 2004.

A Proofs

A.1 Proposition 1

PROPOSITION 1: *Given the dual variable λ , for each i and j , the optimal k^* is determined by $k^* = \arg \max_k (r_{ijk} - \lambda c_k)$. Consequently, $x_{ijk^*} = 1$.*

PROOF When the dual variable λ is known, the optimization problem can be reformulated into solving Equation 17. From this, we can derive the following:

$$\begin{aligned}
L(X, \lambda) &= \max \sum_{i,j} \sum_k r_{ijk} x_{ijk} + \lambda \left(C - \sum_{i,j} \sum_k c_k x_{ijk} \right) \\
&= \max \sum_{i,j} \sum_k (r_{ijk} - \lambda c_k) x_{ijk} + \lambda C \\
&\equiv \max \sum_{i,j} \sum_k (r_{ijk} - \lambda c_k) x_{ijk} \\
&\equiv \max \sum_k (r_{ijk} - \lambda c_k) x_{ijk} \quad \forall i, j
\end{aligned} \tag{21}$$

For each i, j , find the k that maximizes $(r_{ijk} - \lambda c_k)$:

$$k^* = \arg \max_k (r_{ijk} - \lambda c_k) \tag{22}$$

Then set:

$$x_{ijk^*} = 1 \tag{23}$$

The remaining $x_{ijk} = 0$ (for $k \neq k^*$).

A.2 Proposition 2

PROPOSITION 2: *The function $g(\lambda) = \sum_{i,j} \sum_k c_k \cdot x_{ijk} - C$ is a monotone non-increasing function of λ .*

PROOF

$$\begin{aligned}
g(\lambda) &= \sum_{i,j} \sum_k c_k x_{ijk} - C \\
&= \sum_{i,j} \sum_{k^*} c_{k^*} - C, \quad k^* = \arg \max_k (r_{ijk} - \lambda c_k)
\end{aligned} \tag{24}$$

Assume that $0 < \lambda_1 < \lambda_2$. For any given dimension i, j , let the corresponding optimal indices be k_1 and k_2 for λ_1 and λ_2 , respectively. According to the maximum value relationship, we have:

$$r_{k_1} - \lambda_1 c_{k_1} \geq r_{k_2} - \lambda_1 c_{k_2} \tag{25}$$

$$r_{k_2} - \lambda_2 c_{k_2} \geq r_{k_1} - \lambda_2 c_{k_1} \tag{26}$$

By performing an additive transformation on 25 and 26, we obtain:

$$(\lambda_2 - \lambda_1)(c_{k_1} - c_{k_2}) \geq 0 \tag{27}$$

Therefore, it follows that $c_{k_1} \geq c_{k_2}$. Consequently, we have:

$$\sum_{i,j} c_{k_1} - b \geq \sum_{i,j} c_{k_2} - b \implies g(\lambda_1) \geq g(\lambda_2) \tag{28}$$

Thus, the function $g(\lambda)$ is monotonically non-increasing. This property allows us to employ a binary search method to update the dual variable λ .

B Implementation details

We implemented UBTM and all baseline models using Python 3.6 and TensorFlow 1.7.0. During model training, we utilized the Adam optimizer and applied gradient clipping to stabilize the training process. To prevent overfitting, we incorporated batch normalization and a dropout rate of 0.2. For evaluation, we calculated the AUC with a batch size of 8196. All experiments were conducted on an NVIDIA A10 GPU and an Intel(R) Xeon(R) Platinum 8352Y CPU @ 2.20GHz.

Received 18 November 2024; revised XX XX 2024; accepted XX XX 2024